**Abstract** Two-photon stereolithography (TPS) provides many advantages for achieving two-dimensional (2D) and three-dimensional (3D) micrometer-scale polymeric, ceramic and metallic structures applicable to complicated optical and neo-electronic microdevices. In the fabrication of high-resolution 3D microstructures, TPS has significant advantages over conventional microelectromechanical system (MEMS) processing, which involves time-consuming multistep indirect fabrication processes. Many studies have recently been made to develop and improve the TPS process, focusing on creating greater efficiency, higher resolution, and greater productivity, which are essential requirements of a practical TPS process. For the first time, an artistic microstructure has recently been successfully produced with an ultraprecise spatial resolution, sub-30 nm nanofibers, 3D multilayer imprint stamps for mass production, and ceramic 3D microstructures. In this review, we report the progress of two-photon polymerization based on 3D microfabrication, including the results obtained from the original research. This report is presented in three sections: improvement of resolution, precise design schemes, and applications of 3D microstructures.

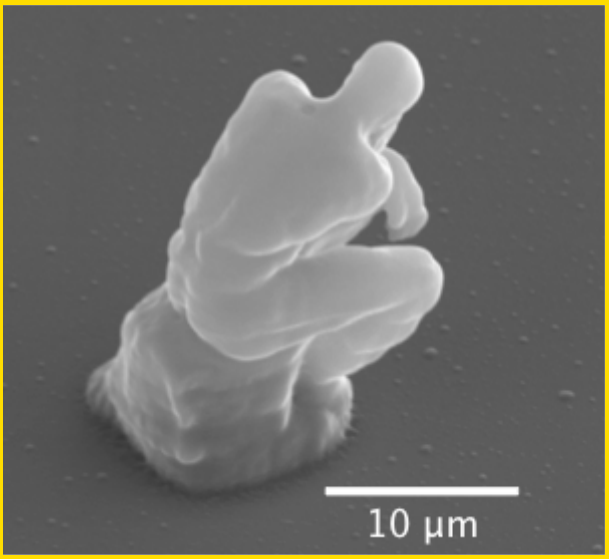


Precise micro 3D pattern fabricated by two-photon lithography.



# Two-photon stereolithography for realizing ultraprecise three-dimensional nano/microdevices

*Sang-Hu Park*[1], *Dong-Yol Yang*[2], *and Kwang-Sup Lee*[3,*]

[1] School of Mechanical Engineering, Pusan National University, Busan 609-735, Korea
[2] Department of Mechanical Engineering, Korea Advanced Institute of Science & Technology, Daejeon 305-701, Korea
[3] Department of Advanced Materials, Hannam University, Daejeon 305-811, Korea

Received: 16 July 2008, Revised: 18 August 2008, Accepted: 21 August 2008
Published online: 24 November 2008

**Key words:** Two-photon stereolithography, photosensitizers, voxels, miniaturization, microdevice.

**PACS:** 81.16.Nd, 85.60.-q, 85.85.+j, 87.85.va

## 1. Introduction

Advances in microfabrication technology have made it possible to provide other emerging technologies, such as biochips and photonic crystals, with many innovative products ranging from high-density integrated circuits, high-definition display, and information storage devices. The growing demand for much higher densities of integration, less power consumption, better performance, and a reduction in fabrication cost remain the salient issues behind the continuous trend in downsizing the dimensions of devices. In most of these cases, fabrication technology continues to be the prerequisite for the success of these developments.

Among the various microfabrication technologies available, two-photon stereolithography (TPS) based on photopolymerization has been considered as a unique process for the realization of three-dimensional (3D) microstructures that are required in optical and electronic applications [1–9]. Furthermore, TPS offers numerous advantages over conventional microfabrication processes used in the

* Corresponding author: e-mail: kslee@hannam.ac.kr

semiconductor industry, which generally requires complicated processing steps and incurs a high cost [10–14]. The major characteristics of TPS can be briefly described as (i) direct fabrication of microstructures without use of any photomask, (ii) high resolution near to 100 nm can be achieved to sub-100 nm using special agents such as a radical quencher, (iii) realization of true 3D microstructures by the accumulation of layers, and (iv) various engineering materials such as polymers, ceramics, metals and hybrid materials can be utilized in the TPS [15–21]. For this reason, many researchers have devoted considerable effort to developing the TPS process, and have reported their research results on the fabrication of high-functional 3D devices using TPS [22–27].

Historically, TPS began with the direct fabrication technology of 3D structures first introduced in 1981 by Kodama [28] and further developed by subsequent groups [29, 30] as the rapid technique of stereolithography (SL). Micro-SL (μ-SL) was then developed by increasing its resolution, reaching up to one or two micrometers [31–34]. While TPS is derived from the earlier SL techniques, and shares the same principles, it differs from these in the dimensions of the fabricated structures. Although conventional micromachining processes generally utilize a subtractive method in fabrication, μ-SL uses an additive approach, which enables the direct fabrication of complex 3D microstructures [35]. However, there are limitations to μ-SL in terms of the spatial resolution of fabricated structures. The minimum thickness of layers is inevitably affected by the viscosity and surface tension of the resin, because a thin layer of resin is generally covered by the elevating method along the normal direction of structures for the creation of another layer [30]. Therefore, it is very difficult to use μ-SL to fabricate ultraprecise microstructures that have a nanodetail or submicrometer scale. However, these problems have been easily resolved by using two-photon polymerization. Since this differs from single-photon polymerization, a very narrow and local region inside the focal plane (in which a very high intensive laser beam is focused) is polymerized via two-photon absorption (TPA). Therefore, a resolution of near 100 nm can be achieved by the TPA.

While a significant amount of research has recently been reported on TPS, some technical issues and questions remain unresolved for practical use in nanomicrofabrication. In this review, we will discuss the recent progress of TPS, focusing on the improvement of resolution, effective fabrication, and potential applications. These are still important issues in the field of TPS.

## 2. Two-photon stereolithography based on photopolymerization

### *2.1. Mechanism of two-photon polymerization*

Recently, many studies involving the absorption of multiple photons into a substance followed by a photochemical change have been performed. Photochemical processes involving the absorption of multiple photons are non-linear in nature, and can only be observed under the high intensities of a laser beam [15, 36]. Multiphoton absorbed excitation has come to play an important role in microfabrication. TPA is one of the popular multiple-photon excitation methods wherein an electron transits from a low energy level to a higher energy level by the simultaneous absorption of two photons. In the simultaneous TPA that has a virtual intermediate stage during excitation, the first excited stage becomes populated by the absorption of the first photon. The stage then typically absorbs the second photon during the lifetime of within $10^{-4}$ to $10^{-9}$ s [37, 38].

When the energy of a photon is given as $h\omega$, where $h$and $\omega$ indicate Planck's constant divided by $2\pi$ and the light angular frequency, respectively, the electron can be transited by absorbing the energy gap, $h\omega = E_2 - E_1$, where $E_2$and $E_1$are the energy level of the upper and lower energy levels, respectively. In the case of two-photon polymerization the photosensitization is brought about by the simultaneously absorbed two photons by a two-photon chromophore. A Ti:sapphire laser is generally used as a source of light for two-photon polymerization due to the generation of super-high power pulses with widths of several tens of femtoseconds (fs). Furthermore, the Ti:sapphire fs-laser is very useful in the case of TPS, because it has a center wavelength of about 780 nm, half of which is close to the critical wavelength for the polymerization of ultraviolet (UV) curable resins. This allows easy control of threshold energy for polymerization in the TPS [36]. Also, Farsari et al. [39] showed the possibility of TPA at a wavelength of 1028 nm (operating wavelength of fs laser) for a TPA dye with one-photon activity between 450–550 nm. Furthermore, three-photon polymerization was demonstrated for the first time by the same research team to open the road for achieving higher resolution; however, the highest resolution, reaching 500 nm, was achieved by the three-photon polymerization [40].

An alternative way for polymerization induced by two-photon absorption is cationic polymerization process. In this process, the photoinitiator generates an acid with a spatial resolution by absorption of near-UV light. Then, the latent image is crosslinked by chain reaction in a postbaking process. A thick film of SU-8 negative photoresist is generally used in the cationic polymerization; therefore, this eases the sample handing and operations during the direct writing process. By this means, complex and physically discontinuous shapes can be realized successfully using this polymerization process [41].

### *2.2. Optical laser system and its operation*

Generally, a mode-locked Ti:sapphire laser is used as a beam source, having a wavelength of 780 nm, a repetition of 80 MHz, and a pulse width of less than 100 fs. The beam is tightly focused using an objective lens (NA, numerical

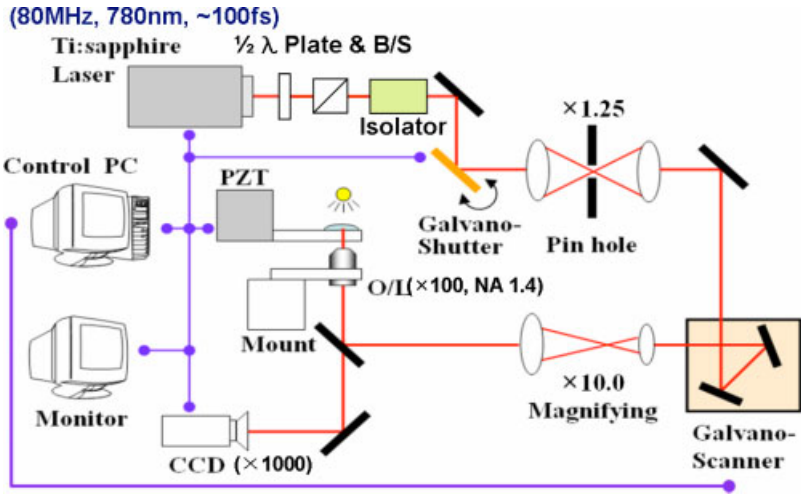


**Figure 1** (online color at: www.lpr-journal.org) Schematic diagram of a laser-optical system setup.

aperture of 1.4 and magnification of 60 times) and is positioned along the out-of-plane ($z$-axis) direction using a piezoelectric stage and along the inplane ($x$–$y$ axis) direction using a galvano-mirror set. Recently, for large-area fabrication within several hundred μm, a stage system has often been used rather than the glavano-scanner to control a focused beam position. In this case, the closely focused beam is fixed and a plate is then moved. The exposing time of the beam is controlled by a glavano-shutter with a stable response time of 1 ms. A resolution of beam positioning is dependent on the capability of stages and scanners. The shutter, scanner, and stage are controlled by a computer system, and a highly magnifying charge-coupled device (CCD) camera can be used to monitor the fabrication process. A schematic illustration is shown in Fig. 1 [42, 43].

For the fabrication of a 3D microstructure using the TPS process, 3D stereolithography data are sliced into many layers along the $z$-axis to generate 2D beam-scanning paths. A sliced layer of a 3D microstructure is polymerized along the scanning paths of a laser beam. A further layer is then fabricated after translating the location of a beam spot along the $z$-axis by using the stage, and is attached to the previously solidified lower layers. These procedures are continuously repeated until the design of the 3D microstructure is completed. After the fabrication, unpolymerized liquid-state resins (monomers) are eliminated using several rinsing solvent droplets (generally, ethanol).

## 3. What is the end of the smallest feature size in TPS?

The improvement of spatial resolution is one of the key issues in the development of TPS, because of the competition with various nanofabrication processes that have very high resolutions, such as electron-beam lithography, nanoimprint lithography, and focused ion-beam lithography. Recently, various research studies have reported the reduction of the lateral feature size, reaching less than 100 nm, by intentionally introducing radical quenchers into photocurable resins. Takada et al. [44] reduced the feature size down to about 65 nm, and Park et al. [45] revealed line patterns that are around 95 nm wide. They demonstrated the tendency of voxel-size reduction by increasing the amount of radical quenchers in a resin. However, the addition of radical quenchers could result in an increase of threshold for two-photon polymerization. Also, it is generally known that the mechanical strength of polymers depends on the length of polymerized chains. Therefore, by adding a radical quencher, the voxel-size reduction causes the low mechanical strength of a polymerized structure due to its low molecular weight. As such, a microstructure with a low mechanical strength is easily distorted by the surface tension of a rinsing material in a developing process [45].

In the TPS, the resolution of microstructures is determined by the size of a voxel (volumetric pixel) that is the minimum unit of a feature. Voxels are generated depending on the laser power and exposure time, and their sizes can be estimated theoretically as shown in Eqs. (1) to (2) [43]:

$$d(P,t,\mathrm{NA}) = \frac{\lambda}{\pi \tan\left(\sin^{-1}(\mathrm{NA}/n)\right)} \times \left[\ln\left(\frac{4\pi^2 P^2 \cdot t \cdot \left[\tan\left(\sin^{-1}(\mathrm{NA}/n)\right)\right]^4}{E_{\mathrm{th}} \cdot \lambda^4}\right)\right]^{1/2}, \quad (1)$$

$$l(P,t,\mathrm{NA}) = 2z = \frac{2\lambda}{\pi \left[\tan\left(\sin^{-1}(\mathrm{NA}/n)\right)\right]^2} \times \left[\left(\frac{4\pi^2 P^2 \cdot t \cdot \left[\tan\left(\sin^{-1}(\mathrm{NA}/n)\right)\right]^4}{\lambda^4 \cdot E_{\mathrm{th}}}\right)^{1/2} - 1\right]^{1/2}, \quad (2)$$

where $d$, $l$, $E_{th}$, $P$, $t$, NA, and $n$ represent the voxel diameter, voxel length, threshold energy for polymerization, laser power, exposure time, numerical aperture of an objective lens, and the refractive index, respectively. As shown in Eqs. (1) and (2), while the dimension of a voxel can be minimized by optimizing the laser dose, the limit of a reso-

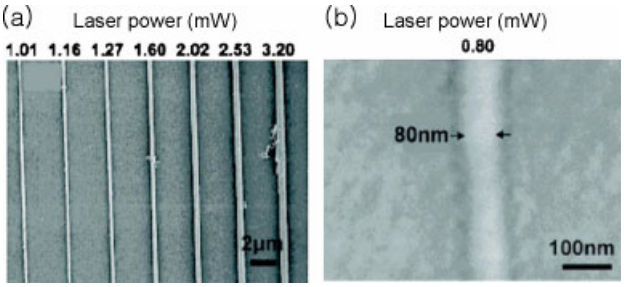


**Figure 2** Scanning electronic microscopy (SEM) images of (a) a pattern fabricated by using different laser powers from 1.01 mW to 3.20 mW at a linear scan speed of 50 μm/s. (b) Magnified SEM image of the pattern having an 80 nm width. Reprinted with permission from [38].

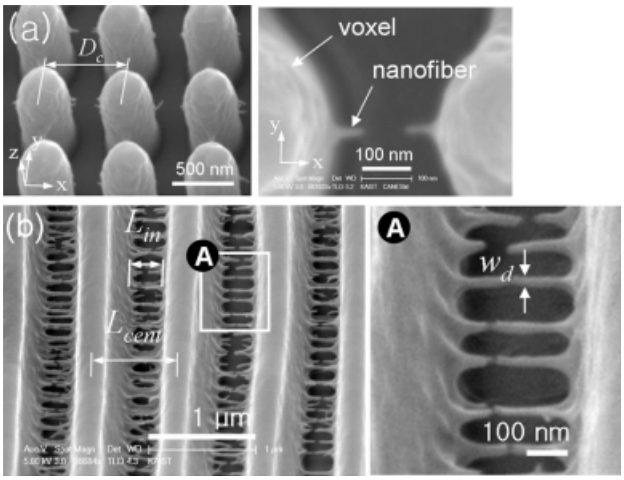


**Figure 3** (a) SEM images of fabricated voxels with the critical distance (700 nm); dim nanofibers were generated near the voxels. (b) Well-generated nanofibers between polymer lines. The distance between lines was about 270 nm. Reprinted with permission from [39].

lution is known to be approximately 100 nm in the lateral size of a voxel [19, 23, 43].

Recently, Xing et al. [46] reported a lateral spatial resolution of 80 nm by using a highly sensitive initiator (9,10-bispentyloxy-2,7-bis[2-(4-dimethylaminophenyl)-vinyl]anthracene) (BPDPA), which contributes to a low threshold and short exposure time. Exposure time influences the number of radicals generated by two-photon absorption. This means that a low threshold for two-photon-induced polymerization would reduce the size of the region where radicals are initially generated. Furthermore, a short exposure time should decrease the number and diffusion of radicals, resulting in ultralocalized polymerization in a small region. For this reason, a highly sensitive initiator could contribute by improving a resolution with a low threshold and short exposure time. Figs. 2a and b show the fabricated results using a highly sensitive initiator and a short exposure time.

The repolymerization technique is an alternative method used to reduce the feature size in the TPS. Three different regions within polymerization: (i) a fully polymerized region with high molecular weight (solid state), (ii) a weakly polymerized region with low molecular weight (solid-liquid state), and (iii) an unpolymerized region (liquid state) [47, 48]. Generally, regions (ii) and (iii) are removed by rinsing materials in a development process. However, region (ii) could be utilized to generate ultrafine features that have less than 30 nm in lateral size by repolymerization. Park et al. [47] fabricated a bunch of 22-nm diameter nanofibers by using the weakly polymerized region. For the generation of nanofibers, they proposed a long-exposure technique (LET). The lateral size of a voxel increased steeply up to a 1 s exposure, and then increased gently up to a 6 s exposure, with a mixture of SCR 500 (JSR) and photosensitizers of 0.1 wt% (4,4'-(1E,1'E)-2.2'-(9,9-bis(4-(octyloxy)phenyl)-9H-fluorene-2,7-diyl)-bis(ethene-2,1-diyl)bis(N,N-diphenylaniline)). Employing the LET, region-(ii) is widely extended around the voxels by the diffusion of radicals, and nanofibers were generated according to the interval between adjacent voxels (see Fig. 3a). When the interval was significantly larger than a critical value, the coupling nanofibers did not appear since there was no overlap between voxels and lines in region (ii). In the previous work [47], the critical distance was about 700 nm. In the case where the weakly polymerized regions overlapped, the low-density short-chained polymers in region (ii) were transformed to highly dense, high-weight polymers via repolymerization induced by the repeated exposure of the laser beam. Fig. 3b shows the well-generated nanofibers using the LET. The repolymerized long-chain polymers are not easily eliminated in the developing process due to their improved mechanical strength.

Other approaches for the generation of nanofibers in the weakly polymerized region have been reported [49], where thick lines were fabricated, and thin fibers of less than 30 nm were then generated along the perpendicular direction of the thick-line patterns via the high scan speed of a tightly focused beam. The feature sizes were dependent on the incident laser power and the scan speed of laser focus. At a certain laser power, the nanofibers became thinner by means of repolymerization when the scan speed was increased to reach a certain limit, as shown in Figs. 4a and 4b.

## 4. Effective fabrication of 3D microstructures

### *4.1. Multipath scanning method*

Despite the powerful merits of TPS in 3D microfabrication, effective and precise fabrication is still an issue to be resolved in terms of practical use. One of the barriers to achieving precise fabrication is known to be the deformation of 3D microstructures during the developing process. The major cause of pattern collapse is recognized as a cohesive force induced by the surface tension of a rinsing

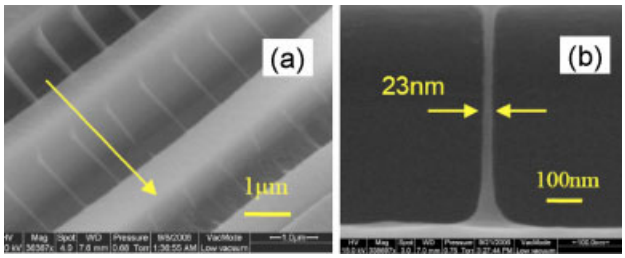


**Figure 4** (online color at: www.lpr-journal.org) (a) SEM images of suspended nanofibers between polymer supports. The fibers thinned down when the scan speed was accelerated in the direction indicated by the arrow. (b) Magnified image of nanofiber having 23 nm in width. Reprinted with permission from [40].

material [50]. The driving force for collapse during a drying step of the rinsing material can be expressed by the Young–Laplace pressure ($\Delta P$), $\Delta P = \sigma(R_1^{-1} + R_2^{-1})$, where the symbols represent the negative pressure difference, the surface tension ($\sigma$) of a rinsing material, and the two radii ($R_1$ and $R_2$) of the surface curvature between structures, respectively. From this equation, a rinsing material that has a low surface tension can be applied to allow a reduction of the collapse force in the development process. However, this application is more expensive. To overcome this problem, increasing the mechanical strength of a pattern itself is essentially required.

Multipath scanning (MPS) is an alternative method used for the effective and precise reinforcement of the mechanical strength of 3D microstructures without the need to reduce the resolution, as illustrated in Fig. 5a [51]. The multipaths can be constructed from the sliced contour data of a 3D microstructure by using a Voronoi diagram. Offsetting was then carried out to generate a new internal scanning path. By repeating this procedure, more than three scanning paths were obtained with precisely controlled offset amounts. Therefore, the target thickness of a feature for sufficient strength could be readily obtained via the control of a number of contours and offset amounts (see Fig. 5b). Using the MPS method, a more complex 3D microstructure, 'the thinker' was created with a height of 20 μm and a width of 12 μm (see Fig. 5c). Since the creation of 'the thinker' designed by Rodin in 1880, this may be the first replica of 'the thinker' in microscale. For the fabrication, double scanning paths were used with an offset of 150 nm, under the conditions of a 40 mW laser power and 1 ms per voxel exposure time. As shown in Fig. 5c, the fine details of the muscles, posture, and appearance were realized using the MPS. Determining a relationship between the mechanical strength and pattern collapse demonstrates the importance of the precise fabrication of 3D microstuctures.

## *4.2. Subregional slicing method*

One of the distinguishable merits of TPS compared to other nano/microfabrication processes is its ability to fabricate a

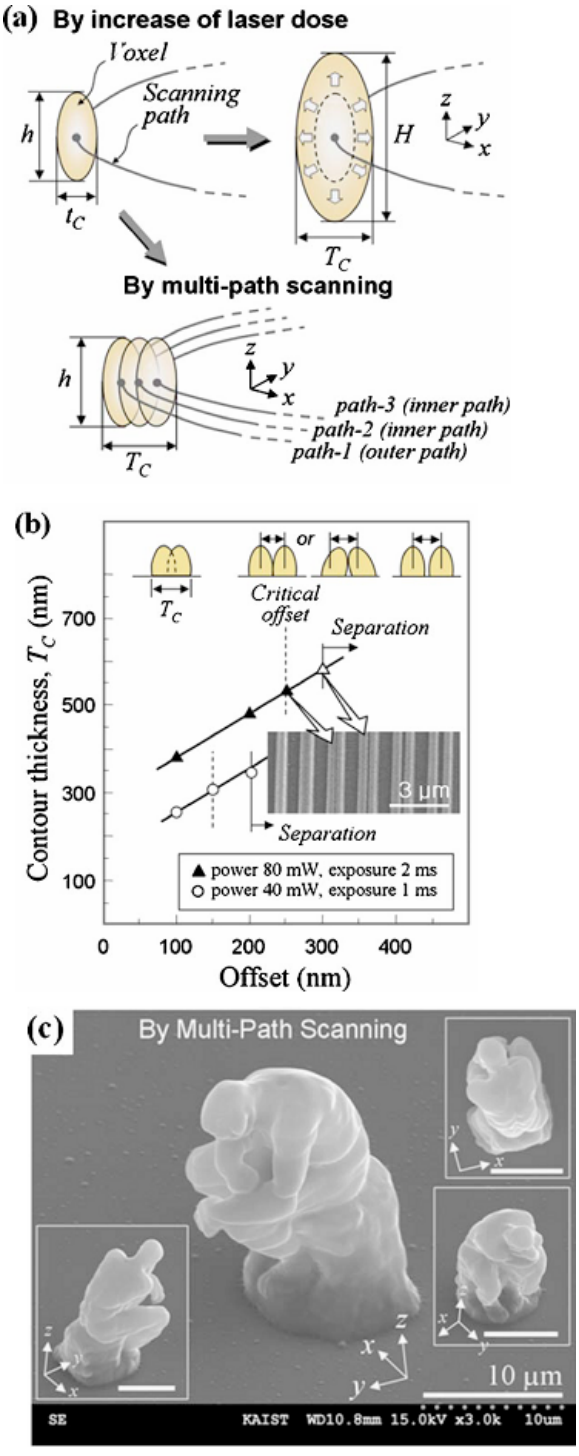


**Figure 5** (online color at: www.lpr-journal.org) (a) Illustration of difference between two approaches for increasing contour thickness; by increase of laser dose and multipath scanning method. In the case of multipath scanning, only the contour thickness becomes thicker depending on the offset and number of paths. (b) The variation of the contour thickness versus offset amount under the conditions of 40 mW and 80 mW laser power, respectively. (c) Successfully fabricated micro-"the thinker" that is about 20 μm tall. Reprinted with permission from [43].

3D arbitrary shape. However, when the 3D microstructure has almost flat areas that are parallel to the slicing planes, a very thin layer thickness is required in order to ensure that all layers are connected to each other. This process, however, significantly increases the fabrication time. The contour scanning method (CSM) is a more effective method compared to the raster scanning method (RSM) [15]. In the CSM, 3D microstructures are fabricated by curing only their contour shells rather than the full polymerization of whole structures as used in the RSM method. For CSM, all adjacent layers should be connected together to form the fully closed shell of a 3D microstructure and it is essential for all the voxels to overlap each other in two adjacent layers. Generally, in order to avoid layer separation caused by a layer thickness that is too large, a suitable layer thickness is determined by considering the geometric slope of a microstructure. A suitable layer can be obtained by experimental and theoretical approaches [52]. To resolve this problem in TPS, two different slicing methods have recently been reported.

The first of these is the subregional slicing method (SSM), which was considered to be an effective method to reduce processing time with high precision. In the SSM, a 3D microstructure was divided into several subregions by considering the structure's geometrical shape or slope. Suitable slicing thicknesses were then applied to each subregion of the microstructure. The total number of sliced layers could therefore be reduced by using the SSM, while the precision of the microstructures was not diminished in comparison to the uniform slicing method, where the layers are finely sliced (USM).

### *4.3. Two-dimensional slicing method*

The second approach, the two-dimensional slicing method (TSM), was proposed to cope with the manufacture of 3D microstructures that have almost planar regions and very gentle slopes [53]. TSM has two slicing data: horizontally sliced data and vertically sliced data. In the TSM, a critical slicing angle according to the shape of a microstructure is specified for preparing two kinds of scanning data. In the primary slicing phase, a 3D polyhedral model is divided into two subdomains by considering the shape angle of each triangular face. The subdomains are then sliced along two different directions perpendicular to each other, as illustrated in Fig. 6a. By using the TSM, a complex 3D microstructure has been successfully realized, as shown in Fig. 6b.

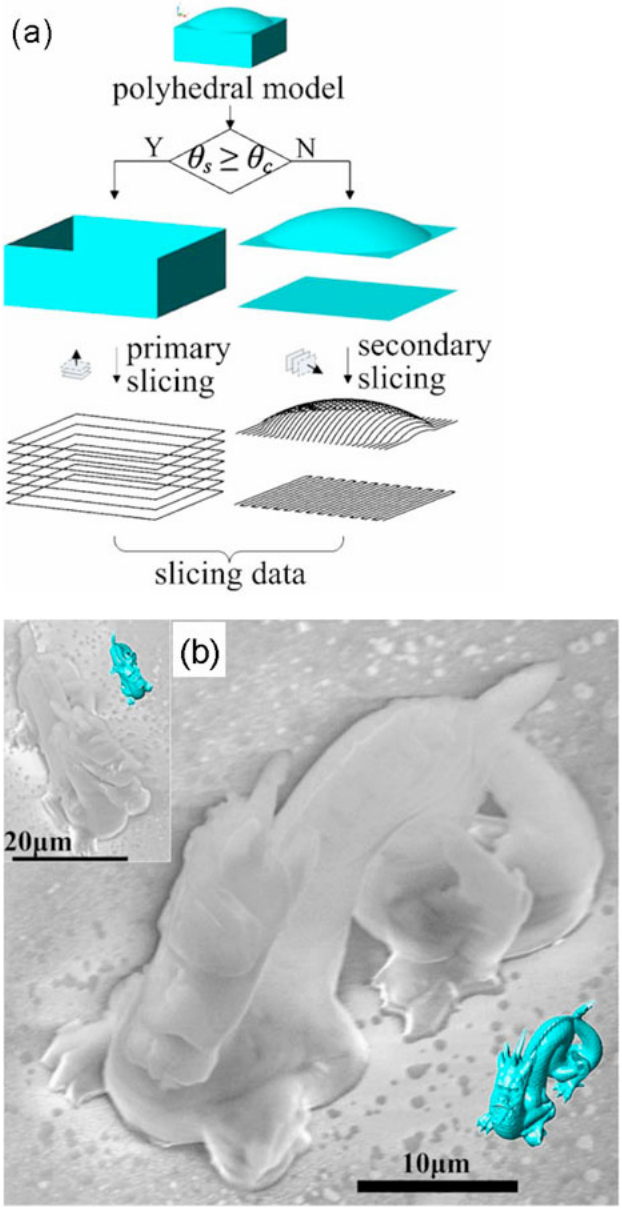


**Figure 6** (online color at: www.lpr-journal.org) (a) Schematic procedure flow of the two-dimensional slicing method (TSM). The slicing data are composed of two directional slicing data. (b) SEM image of microdragon fabricated by TSM, which has gentle slops on its top. Reprinted with permission from [45].

## 5. Applications of TPS

### *5.1. Implantation of 3D microstructures*

During the past ten years, rapid progress in 3D microfabrication has been made using TPS. To date, a variety of 3D applications have been reported for high-functional use in diverse research fields such as optics, mechanics, and biotechnology. Despite this promising potential of TPS, it is still difficult to directly fabricate 3D microstructures on an opaque material or within a large-area practical microsystem. Even when direct fabrication is possible using TPS, the nanoscale control of a tightly focused beam along a large-area of more than 1 mm is generally cost prohibitive. This is one of the obstructions inhibiting the practical use

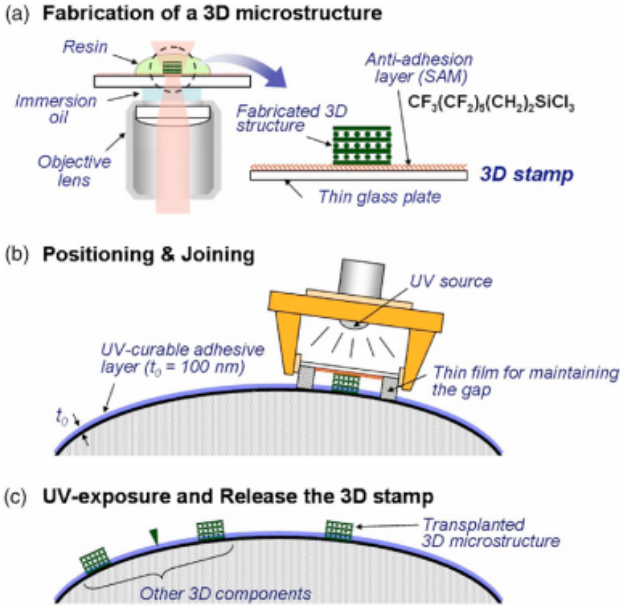


**Figure 7** (online color at: www.lpr-journal.org) Illustration of three steps of contact print lithography (CPL); (a) fabrication of a stamp using two-photon polymerization for implantation into another surface; (b) positioning and joining the 3D microstructures on a surface by UV curing; (c) final shape after implantation by the CPL. Reprinted with permission from [46].

of TPS as a nanofabrication process. As one of the possibilities to resolve this issue, a contact-print lithography (CPL) method has been proposed [54].

There are three basic steps involved in transplanting 3D microstructures on a large-size substrate, as schematically illustrated in Figs. 7a–c. Firstly, a 3D stamp is prepared using TPS; fabrication of 3D microstructures on a glass plate. Prior to 3D microfabrication, a self-assembled monolayer (SAM) is deposited on a glass plate (the stamp surface) to reduce the adhesive force between the 3D microstructure and the glass plate. The stamp is then precisely positioned on a target substrate coated with a thin ultraviolet (UV)-curable, adhesive layer. Next, the bonding layer is cured by UV light in order to bond the 3D microstructure onto the substrate and the glass plate is then carefully removed. Figs. 8a and b show successfully transplanted microstructures on an opaque substrate, in this case silicon wafer used. As shown in the figures, the edge size of the top surface in the transplanted woodpile is also 9 µm, compared to the edge size of the bottom surface of the structure before CPL.

## *5.2. Net shape manufacturing of 3D ceramic microstructures and molds*

When devices are used in harsh environments, they must be able to withstand high temperatures and chemical corrosion, and they must have a high mechanical strength. Therefore, there has been an increasing demand in microfabrication for

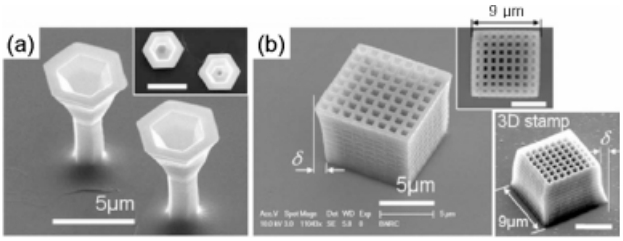


**Figure 8** SEM images of transplanted 3D microstructures; (a) well-standing pillars with hexagon heads, and (b) a woodpile structure. The inserts show the top view of implanted structures. Reprinted with permission from [46].

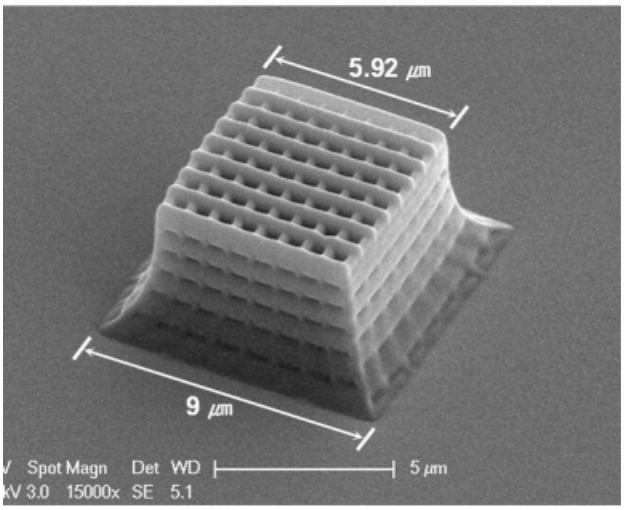


**Figure 9** SEM image of a woodpile after pyrolysis. The structure was anisotropically reduced to the dimension of 5.92 µm from 9.0 µm at the top length. Reprinted with permission from [47].

new engineering materials that have advantages in terms of their high-value properties. Recently, a precise fabrication method has been reported for 3D ceramic microstructures using a two-photon crosslinking process (TPCL) [19, 55]. This process paves the way for the direct fabrication of a complicated 3D microstructure with several hundred nanometer detail. This may become an important process for the fabrication of various ceramic applications in the near future. However, a severe shrinkage problem arises with this process, which inevitably occurs during the pyrolysis of polymeric ceramic precursors. This problem is considered to be an obstacle for the practical use of this process. It is well known that the cause of volume shrinkage occurs in the pyrolytic transformation from a low-density polymer to a high-density ceramic (see Fig. 9). Another recent work on direct patterning of inorganic material $TiO_2$ having high refractive index was reported for the promising fabrication of photonic crystals [56]. In this case, 50% shrinkage of volume was observed during thermal treatment to increase the refractivity of $TiO_2$; so the shrinkage problem is still a

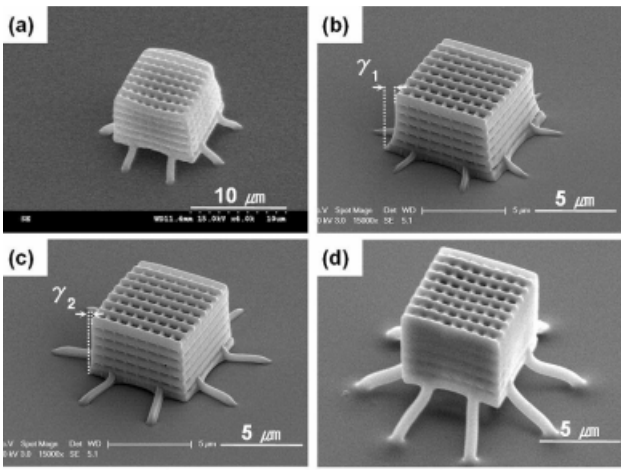


**Figure 10** (a)–(d) Two-photon crosslinked woodpile structures with various shrinkage guiders. The structures were reduced isotropically by the guiders. As shown in (b) and (c), the gap ($\gamma_2$) between top and bottom in (c) was much smaller than the gap ($\gamma_1$) in (b) due to the optimized guider length. Reprinted with permission from [47].

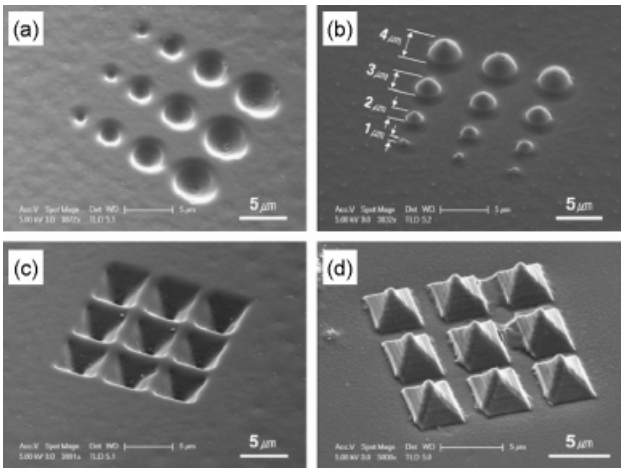


**Figure 11** SEM images of fabricated PDMS molds (a and c) and replicated SiCN ceramic structures (b and d) from the molds. Reprinted with permission from [48].

challenging issue for direct patterning of inorganic materials.

To control the amount of shrinkage during pyrolysis or thermal treatment, a shrinkage guider was introduced. Using this approach, the fabrication of precise 3D ceramic microstructures was possible without any shape distortion, even when a large amount of shrinkage occurred. Figs. 10a–d show the fabricated results depending on various lengths of shrinkage guiders. The length of the guiders could be described as $\delta/(1-\varepsilon-\cos\theta)$, where $\varepsilon$ is the shrinkage rate, $\delta$ is the horizontal displacement on the bottom contour after pyrolysis, and $\theta$ is the inclination angle of a guider, as illustrated in the insert of Fig. 10a. From the results, it was confirmed that shrinkage-guiding is an effective method for the fabrication of precise 3D ceramic microstructures.

Another method has been reported for the fabrication of 3D SiCN-based ceramic molds for the stamp used in a hot-embossing process [57]. The ceramic stamp is fabricated by a sequential process involving the fabrication of polymer master patterns and PDMS molds, micromolding using a preceramic polymer, and a pyrolysis process. After the fabrication of 3D master patterns by TPS, a casting process is used to obtain a concave PDMS mold. The ceramic precursor is then spread onto the patterned surface of the PDMS molds that are fabricated from two master patterns. Viscous polyvinylsilazane (Kion® VL20) is used as a precursor of the SiCN ceramic. The excess polymer is scraped away using a piece of flat PDMS, leaving a filled PDMS mold. The filled mold is then brought into contact with a Si wafer, and the polymeric precursor is cured under a UV-light for 20 min at an intensity of 10 mW/cm$^2$. The PDMS mold is then removed either by peeling it from the substrate or by dissolving it with a 1.0 M tetrabutylammonium fluoride solution in tetrahydrofuran at room temperature. Both methods were performed without producing defects in the polymeric structures. All of the processes were carried out in an inert gas atmosphere in order to avoid exposure to moisture. The patterned polymeric microstructures were then transferred to a tube furnace and heated to 800 °C at a rate of 2 °C/min. During the entire process, 3D SiCN ceramic micropatterns were obtained due to the phase transition during pyrolysis. Figs. 11a and c show PDMS molds in which master patterns were fabricated using the TPS process, while Figs. 11b and d show SiCN ceramic structures created by microtransfer molding using PDMS molds. In the latter case, various patterns can be fabricated within a submicrometer resolution, providing a considerable improvement compared to earlier research in the area of fabrication of ceramic microstructures.

## 6. Conclusions

TPS has many advantages as a technique for the direct fabrication of complex 3D structures on a scale of several micrometers that might be difficult to be obtained by using general miniaturization technologies. In this review, an outline is presented of a number of research studies that are related to the improvement of fabrication efficiency, precise fabrication, and applications. While there has been a great deal of achievement in the development of TPS, challenging issues still need to be explored for the practical use of TPS as a promising nano/microfabrication process: reliability of TPS, improvement of TPA materials, and large-area fabrication methods. However, in the near future, we expect that the TPS will take a position as a powerful process for the fabrication of 3D nano/microdevices applicable to diverse research fields.

*Acknowledgements* This work was supported by the Korea Foundation for International Cooperation of Science & Technology (No. K20702000013-07E0200-01310). One of the authors (D.-Y. Yang) gives thanks to KOSEF for supporting (M10503000217-05M0300-21700). Also K.-S. Lee gives thanks to the Active Polymer Center for Pattern Integration (KOSEF ERC R11-2007-050-01002-0) and the Asian Office of Aerospace Research and Development (AOARD), USA for their support.

Sang Hu Park, born in 1969, earned his B. S. in mechanical engineering at Pusan National University (Korea) in 1994 and his M. S. and Ph. D. in mechanical engineering at Korea Advanced Institute of Science and Technology (KAIST, Korea) in 1996 and 2006, respectively. From 2001 to the present, he has worked on the development of a new process for 3D nano/microfabrication. He joined the faculty of the School of Mechanical Engineering at Pusan National University in 2007.

Dong-Yol Yang, born in 1950, studied mechanical engineering at Seoul National University (Korea). He received his M. S. and Ph. D. in mechanical engineering at Korea Advanced Institute of Science and Technology (KAIST, Korea) in 1975 and 1978, respectively. He joined the mechanical engineering faculty at KAIST in 1978, also he has been a POSCO professor from 2002 to the present. He is presently a life member of the Korean Academy of Science and Technology, and a member of ASME, KSME, JSTP and CIRP.

Kwang-Sup Lee is the Dean of the College of Life Science and Nanotechnology and Professor of the Department of Advanced Materials at the Hannam University, Korea. He also holds a position as the Research Professor at the Institute for Lasers, Photonics and Biophotonics at the University at Buffalo, SUNY, USA. He received his B. S. degree in chemistry from Hannam University in 1976, an M. S. degree in polymer chemistry from Korea University in 1980, and a doctorate in polymer science from the Freiburg University, Germany in 1984. He was a postdoctoral fellow at the Max-Planck-Institute for Polymer Research from 1985 to 1986 and a visiting professor at the Naval Research Laboratory, USA in 1998. Prof. Lee's research interests lie in the field of photofunctional materials including the synthesis of conjugated organics and polymers, quantum dots, carbon nanotubes, and organic–inorganic hybrid materials and fabrication of device involving them.

## References

[1] S. Maruo, O. Nakamura, and S. Kawata, Three-dimensional microfabrication with two-photon-absorbed photopolymerization, Opt. Lett. **22**, 132–134 (1997).
[2] B. H. Cumpston, S. P. Ananthavel, S. Barlow, D. L. Dyer, J. E. Ehrlich, L. L. Erskine, A. A. Heikal, S. M. Kuebler, I. Y. S. Lee, D. McCord-Maughon, J. Q. Qin, H. Rockel, M. Rumi, X. L. Wu, S. R. Marder, and J. W. Perry, Two photon polymerization initiators for three-dimensional optical data storage and microfabrication, Nature **398**, 51–54 (1999).
[3] S. Maruo, and S. Kawata, Two-photon-absorbed near-infrared photopolymerization for three-dimensional microfabrication, J. Microelectromech. Syst. **7**, 411–415, (1998).
[4] S. Kawata, H. B. Sun, T. Tanaka, and K. Takada, Finer features for functional microdevices, Nature **412**, 697–698 (2001).
[5] J. Serbin, A. Egbert, A. Ostendorf, and B. N. Chichkov, Femtosecond laser-induced two-photon polymerization of inorganic-organic hybrid materials for applications in photonics, Opt. Lett. **28**, 301–303 (2003).
[6] S. Yokoyama, T. Nakahama, H. Miki, and S. Mashiko, Fabrication of three-dimensional microstructure in optical-gain medium using two-photon-induced photopolymerization technique, Thin Solid Films **438**, 452–456 (2003).
[7] S. Klein, A. Barsella, H. Leblond, H. Bulou, A. Fort, C. Andraud, G. Lemercier, J. C. Mulatier, and K. Dorkenoo, Onestep waveguide and optical circuit writing in photopolymerizable materials processed by two-photon absorption, Appl. Phys. Lett. **86**, 211118 (2005).
[8] R. Guo, S. Z. Xiao, X. M. Zhai, J. Li, A. Xia, and W. Huang, Micro lens fabrication by means of femtosecond two photon photopolymerization, Opt. Exp. **14**, 810–816 (2006).
[9] J. Ishihara, K. Komatsu, O. Sugihara, and T. Kaino, Fabrication of three-dimensional calixarene polymer waveguides using two-photon assisted polymerization, Appl. Phys. Lett. **90**, 033511 (2007).
[10] H. B. Sun, K. Takada, and S. Kawata, Elastic force analysis of functional polymer submicrometer oscillators, Appl. Phys. Lett. **79**, 3173–3175 (2001).
[11] S. Maruo, K. Ikuta, and H. Korogi, Force-controllable, optically driven micromachines fabricated by single-step twophoton microstereolithography, J. Micromech. Syst. **12**, 7 (2003).
[12] S. Basu, L. P. Cunningham, G. D. Pins, K. A. Bush, R. Taboada, A. R. Howell, J. Wang, and P. J. Campagnola, Multiphoton excited fabrication of collagen matrixes crosslinked by a modified benzophenone dimer: bioactivity and enzymatic degradation, Biomacromol. **6**, 1465–1474 (2005).
[13] S. Maruo, and H. Inoue, Optically driven viscous micropump using a rotating microdisk, Appl. Phys. Lett. **91**, 084101 (2007).
[14] C. N. LaFratta, J. T. Fourkas, T. Baldacchini, and R. A. Farrer, Multiphoton fabrication, Angew. Chem. Int. Ed. **46**, 6238–6258 (2007).
[15] H. B. Sun, and S. Kawata, Two-photon laser precision microfabrication and its applications to micro-nano devices and systems, J. Lightwave Technol. **21**, 624–633 (2003).

[16] E.-Y. Pan, N.-W. Pu, Y.-P. Tong, and H.-F. Yau, Fabrication of high-aspect-ratio sub-diffraction-limit microstructures by two-photon-absorption photopolymerization, Appl. Phys. B **77**, 485–488 (2003).
[17] X. M. Duan, H. B. Sun, K. Kaneko, and S. Kawata, Two-photon polymerization of metal ions doped acrylate monomers and oligomers for three-dimensional structure fabrication, Thin Solid Films **453–454**, 518–521 (2004).
[18] A. Ishikawa, T. Tanaka, and S. Kawata, Improvement in the reduction of silver ions in aqueous solution using two-photon sensitive dye, Appl. Phys. Lett. **89**, 113102 (2006).
[19] A. T. Pham, T. W. Lim, S. H. Park, D. Y. Yang, K.-S. Lee, and D. P. Kim, Three-dimensional SiCN ceramic structures via nano-stereolithography of inorganic polymer photoresist, Adv. Funct. Mater. **16**, 1235–1241 (2006).
[20] F. Formanek, N. Takeyasu, T. Tanaka, K. Chiyoda, A. Ishikawa, and S. Kawata, Selective electroless plating to fabricate complex three-dimensional metallic micro/nanostructures, Appl. Phys. Lett. **88**, 083110 (2006).
[21] A. Ovsianikov, B. Chichkov, P. Mente, N. A. Monteiro-Riviere, A. Doraiswamy, and R. J. Narayan, Two photon polymerization of polymer-ceramic hybrid materials for transdermal drug delivery, Int. J. Appl. Ceram. Technol. **4**, 22–29 (2007).
[22] P. Galajda, and P. Ormos, Complex micromachines produced and driven by light, Appl. Phys. Lett. **78**, 249–251 (2001).
[23] C. N. Lafratta, T. Baldacchini, R. A. Farrer, J. T. Fourkas, M. C. Teich, B. E. A. Saleh, and M. J. Naughton, Replication of two-photon-polymerized structures with extremely high aspect ratio and large overhangs, J. Phys. Chem. B **108**, 11256–11258 (2004).
[24] R. Guo, Z. Y. Li, Z. W. Jiang, D. J. Yuan, W. H. Huang, and A. D. Xia, Log-pile photonic crystal fabricated by twophoton photopolymerization, J. Opt. A Pure Appl. Opt. **7**, 396–399 (2005).
[25] N. D. Lai, W. P. Liang, J. H. Lin, C. C. Hsu, and C. H. Lin, Fabrication of two- and three-dimensional periodic structures by multiexposure of two-beam interference technique, Opt. Exp. **13**, 9605–9611 (2005).
[26] R. A. Farrer, C. N. LaFratta, L. J. Li, J. Praino, M. J. Naughton, B. E. A. Saleh, M. C. Teich, and J. T. Fourkas, Selective functionalization of 3-D polymer microstructures, J. Am. Chem. Soc. **128**, 1796–1797 (2006).
[27] D. Y. Yang, T. W. Lim, Y. Son, H. J. Kong, K.-S. Lee, D. P. Kim, and S. H. Park, Additive Process using Femto-second Laser for Manufacturing Three-dimensional Nano/Micro-structures, Int. J. Prec. Eng. Manuf. **8**, 63–69 (2007).
[28] H. Kodama, Automatic method for fabricating a 3-dimensional plastic model with photo-hardening polymer, Rev. Sci. Instrum. **52**, 1770–1773 (1981).
[29] T. Katagi, and N. Nakajima, Photoforming applied to fine machining, in: Proceedings of the IEEE MEMS '93, pp. 173–178.
[30] P. F. Jacobs, Stereolithography and other RP&M Technologies – From Rapid Prototyping to Rapid Tooling (ASME Press, New York, 1996).
[31] K. Ikuta, T. Ogata, M. Tsubio, and S. Kojima, Development of mass productive micro stereolithography (Mass-IH process), in: Proceedings of the IEEE MEMS '96, pp. 301–305.
[32] S. Monneret, V. Loubere, and S. Corbel, Microstereolithography using a dynamic mask generator and a noncoherent visible light source, Proc. SPIE **3680**, 553–561 (1999).
[33] L. Beluze, A. Bertsch, and P. Renaud, Microstereolithography: a new process to build complex 3D objects, Proc. SPIE **3680**, 808–817 (1999).
[34] A. Bertsch, P. Bernhard, C. Vogt, and P. Renaud, Rapid prototyping of small size objects, Rapid Prototyping J. **6**, 259–266 (2000).
[35] J. Serbin, and M. Gu, Superprism phenomena in waveguide coupled woodpile structures fabricated by two-photon polymerization, Opt. Exp. **14**, 3563–3568 (2006).
[36] K.-S. Lee, R. H. Kim, D. Y. Yang, and S. H. Park, Advances in 3D nano/microfabrication using two-photon initiated polymerization, Prog. Polym. Sci. **33**, 631–681 (2008).
[37] J. P. Fouassier, Photoinitiation, Photopolymerization, and Photocuring – Fundamentals and Applications (Hanser Publishers, Munich, 1995).
[38] V. K. Varadan, X. Jiang, and V. V. Varadan, Microstereolithography and other Fabrication Techniques for 3D MEMS (John Wiley & Sons, Chichester, 2001).
[39] M. Farsari, G. Filippidis, K. Sambani, T. S. Drakakis, and C. Fotakis, Two-photon polymerization of an eosin y-sensitized acrylate composite, J. Photochem. Photobiol. A **181**, 132–135 (2006).
[40] M. Farsari, G. Filippidis, and C. Fotakis, Fabrication of three-dimensional structures by three-photon polymerization, Opt. Lett. **30**, 3180–3182 (2005).
[41] M. Deubel, G. V. Freymann, M. Wegener, S. Pereira, K. Busch, and C. Soukoulis, Direct laser writing of three-dimensional photonic-crystal templates for telecommunications, Nature Mater. **3**, 444–447 (2004).
[42] K.-S. Lee, R. H. Kim, P. Prabhakaran, D. Y. Yang, T. W. Lim, and S. H. Park, Two-photon stereolithography, J. Nonlin. Opt. Phys. Mater. **16**, 59–73 (2007).
[43] K.-S. Lee, D.-Y. Yang, S. H. Park, and R. H. Kim, Recent developments in two-photon polymerization for 2D and 3D microfabrications, Polym. Adv. Technol. **17**, 72–82 (2006).
[44] K. Takada, H. B. Sun, and S. Kawata, Improved spatial resolution and surface roughness in photopolymerization-based laser nanowriting, Appl. Phys. Lett. **86**, 071122 (2005).
[45] S. H. Park, R. H. Kim, T. W. Lim, D. Y. Yang, and K.-S. Lee, Improvement of spatial resolution in two-photon polymerization using radical quencher, Macromol. Res. **14**, 559–564 (2006).
[46] J.-F. Xing, X.-Z. Dong, W.-Q. Chen, X.-M. Duan, N. Takeyasu, T. Tanaka, and S. Kawata, Improving spatial resolution of two-photon microfabrication by using photoinitiator with high initiating efficiency, Appl. Phys. Lett. **90**, 131106 (2007).
[47] S. H. Park, T. W. Lim, D. Y. Yang, R. H. Kim, and K.-S. Lee, Fabrication of a bunch of sub-30 nm nanofibers contained microchannels using photopolymerization via long exposing technique, Appl. Phys. Lett. **89**, 173133 (2006).
[48] S. Juodkazis, V. Mizeikis, K. K. Seet, M. Miwa, and H. Misawa, Two-photon lithography of nanorods in SU-8 photoresist, Nanotechnology **16**, 846–849 (2005).
[49] D. Tan, Y. Li, F. Qi, H. Yang, Q. Gong, X. Dong, and X. Duan, Reduction in feature size of two-photon poly-

merization using SCR500, Appl. Phys. Lett. **90**, 071106 (2007).
[50] S. H. Park, K. H. Kim, T. W. Lim, D. Y. Yang, and K.-S. Lee, Investigation of three-dimensional pattern collapse owing to surface tension using an imperfection finite element model, Microelectron. Eng. **85**, 432–439 (2008).
[51] D. Y. Yang, S. H. Park, T. W. Lim, H. J. Kong, S. W. Yi, H. K. Yang, and K.-S. Lee, Ultraprecise microproduction of a three-dimensional artistic sculpture by multipath scanning method in two-photon photopolymerization, Appl. Phys. Lett. **90**, 013113 (2007)
[52] S. H. Park, S. H. Lee, D.-Y. Yang, H. J. Kong, and K.-S. Lee, Subregional slicing method to increase 3D nanofabrication efficiency in two-photon polymerization, Appl. Phys. Lett. **87**, 154108 (2005).
[53] C.-Y. Liao, M. Bouriauand, P. L. Baldeck, J.-C. Leon, C. Masclet, and T.-T. Chung, Two-dimensional slicing method to speed up the fabrication of micro-objects based on two-photon polymerization, Appl. Phys. Lett. **91**, 033108 (2007).
[54] S. H. Park, J. H. Jeong, D. K. Choi, K. D. Kim, A. Altun, E. S. Lee, D. Y. Yang, and K.-S. Lee, Adaptive bonding technique for precise assembly of three-dimensional microstructures, Appl. Phys. Lett. **90**, 233109 (2007).
[55] T. W. Lim, Y. Son, D.-Y. Yang, T. A. Pham, D. P. Kim, B. I. Yang, K.-S. Lee, and S. H. Park, Net shape manufacturing of three-dimensional SiCN ceramic microstructures using an isotropic shrinkage method by introducing shrinkage guiders, Int. J. Appl. Ceram. Technol. **5**, 258–264 (2008).
[56] S. Passinger, M. S. M. Saifullah, C. Reinhardt, K. R. V. Subramanian, B. N. Chichkov, and M. E. Welland, Direct 3D patterning of $TiO_2$ using femtosecond laser pulses, Adv. Mater. **19**, 1218–1221 (2007).
[57] T. W. Lim, S. H. Park, D.-Y. Yang, A. T. Pham, D. H. Lee, and D.-P. Kim, Fabrication of three-dimensional SiCN Ceramic structures for effective replication of microstructures, Microelectron. Eng. **83**, 2475–2481 (2006).